Neuron, Vol. 44, 749–757, December 2, 2004, Copyright ©2004 by Cell Press

Shrinkage of Dendritic Spines Associated with Long-Term Depression of Hippocampal Synapses

Report

Qiang Zhou,[1] Koichi J. Homma,[1] and Mu-ming Poo*
Division of Neurobiology
Department of Molecular and Cell Biology
Helen Will Neuroscience Institute
University of California, Berkeley
Berkeley, California 94720

Summary

Activity-induced modification of neuronal connections is essential for the development of the nervous system and may also underlie learning and memory functions of mature brain. Previous studies have shown an increase in dendritic spine density and/or enlargement of spines after the induction of long-term potentiation (LTP). Using two-photon time-lapse imaging of dendritic spines in acute hippocampal slices from neonatal rats, we found that the induction of long-term depression (LTD) by low-frequency stimulation is accompanied by a marked shrinkage of spines, which can be reversed by subsequent high-frequency stimulation that induces LTP. The spine shrinkage requires activation of NMDA receptors and calcineurin, similar to that for LTD. However, spine shrinkage is mediated by cofilin, but not by protein phosphatase 1 (PP1), which is essential for LTD, suggesting that different downstream pathways are involved in spine shrinkage and LTD. This activity-induced spine shrinkage may contribute to activity-dependent elimination of synaptic connections.

Introduction

Dendritic spines are major sites of excitatory synaptic transmission in the central nervous system (Harris, 1999; Nimchinsky et al., 2002; Yuste and Bonhoeffer, 2004). Changes in their density and morphology occur during development (Dailey and Smith, 1996; Fiala et al., 1998; Dunaevsky et al., 1999), learning (Moser et al., 1994; Geinisman, 2000; O'Malley et al., 2000), aging (Uemura, 1980; Jacobs et al., 1997), and various types of mental disorders (Ferrer and Gullotta, 1990; Comery et al., 1997). In mammals, dendritic spines begin to increase in density during the first week after birth and reach the peak in the third week, which corresponds roughly to the peak of synaptogenesis (White et al., 1997; Harris, 1999; Nimchinsky et al., 2002). There is evidence for a subsequent pruning of spines before attaining the mature spine density several months after birth (Wise et al., 1979), a process that may be related to activity-dependent developmental refinement of synaptic connections.

Activity-induced persistent synaptic modifications may involve alterations in both the functional efficacy of synaptic transmission and the structure of neuronal connections. Recent studies using time-lapse two-photon imaging have shown an increased density of dendritic protrusions (spines and filopodia) (Engert and Bonhoeffer, 1999; Maletic-Savatic et al., 1999) or enlargement of the spine head (Matsuzaki et al., 2004) after stimulations that are known to induce LTP. Ultrastructural studies using electron microscopy have produced mixed results: while some groups reported enlargement of the spine head (Fifkova and Van Harreveld, 1977; Desmond and Levy, 1983, 1986a), shortening of the spine neck (Fifkova and Anderson, 1981), and increase in the spine density and the area of postsynaptic densities (PSDs) (Chang and Greenough, 1984; Desmond and Levy, 1986a, 1986b), other groups reported no apparent changes of the above parameters (Lee et al., 1980; Sorra and Harris, 1998; Andersen and Soleng, 1998). Taken together, these studies on LTP-related changes in dendritic spines have raised a number of interesting issues. First, is there any change in spine morphology and density following the induction of LTD? Second, are these changes reversible? Third, what are the cellular signaling events mediating these changes? Finally, are functional modifications associated with LTP/LTD causally related to changes in spine morphology and density? In this study, we have examined some of these issues in acute rat hippocampal slices, taking advantage of time-lapse two-photon imaging that allows observations of morphological changes in the same population of spines.

Results

Dendritic Spines Undergo Shrinkage after LTD Induction

To image dendritic spines, CA1 pyramidal cells were filled with an inert fluorescent dye, calcein, through the whole-cell recording pipette (Figure 1A). Synapses were activated by a glass pipette positioned 20–30 μm away from the imaged spines (Figure 1A). Most of the synapses on the spines in the imaged field can be effectively activated by the nearby stimulating pipette, as evidenced by a rise of Ca^{2+} in the spines (Figure 1B), monitored by Ca^{2+}-sensitive fluorescent dye Oregon Green BAPTA (see Experimental Procedures). About 60%–70% of the spines in the image field were activated by the local stimulation ($n = 8$ neurons). Furthermore, this local rise in Ca^{2+} in the spine can be induced by subthreshold stimulation and is mediated by Ca^{2+} influx through NMDA receptors, as it was abolished by the NMDA blocker APV (50 μM, data not shown).

Two-photon laser scanning microscopy was used to examine the same population of spines repeatedly before and after low-frequency stimulation (LFS, 1 Hz for 15 min) that induced LTD (see Figure 2A). In the absence of LFS, dendritic spines exhibited stable morphology over a period of 1–2 hr, and only a small portion of them had long-lasting changes in their shapes (Figure 1C). Imaging of the same set of dendritic spines showed that many spines exhibited progressive reduction in the

*Correspondence: mpoo@uclink.berkeley.edu
[1]These authors contributed equally to this work.

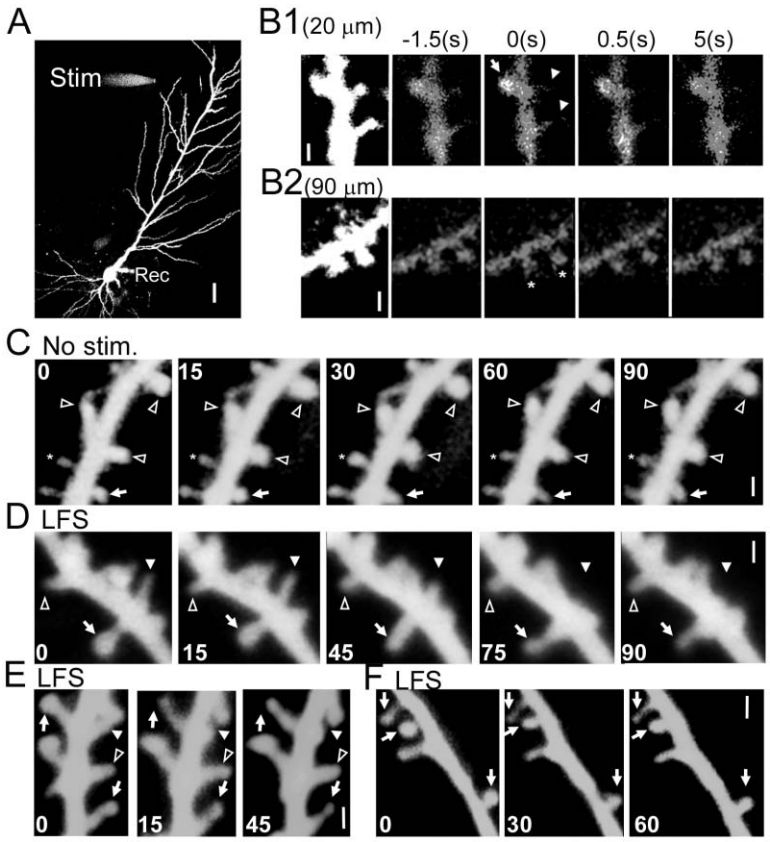

Figure 1. Reduction of the Spine Size Associated with Low-Frequency Stimulation

(A) A low-magnification image of a recorded pyramidal neuron, together with the recording ("Rec") and stimulating ("Stim") electrodes. The image was a 2D projection of a 3D stack of images with 1 μm z step. Scale bar, 20 μm. (B1 and B2) Synaptic activation of spines was observed when they were close to ([B1], 20 μm) but not when they were far from ([B2], 90 μm) the stimulating electrode. Examples depict the morphology of the spines in 2D projections of a 3D z stack of images (first on the left) and changes in $[Ca^{2+}]_i$ (right four images) shown at one focal plane. The numbers above indicate the time of image acquisition, and the stimuli were given at time 0. The spine that exhibited transient $[Ca^{2+}]_i$ elevation at the focal plane was marked by an arrow. Two other spines (arrowheads) at different focal planes also showed transient $[Ca^{2+}]_i$ elevation. The spines that did not show $[Ca^{2+}]_i$ elevation in response to stimulation were marked by *. (C) Spines are largely stable (arrowheads) in the absence of LFS. A small percentage of spines underwent spontaneous shrinkage (arrows). Note that transient changes occurred on some spines (*). (D–F) Persistent reduction in the spine size after LFS. Some spines underwent progressive reduction in the spine head (arrows), while others showed no apparent changes (open arrowheads). A small fraction of spines (E) or filopodia (D) retracted (filled arrowheads). Numbers refer to minutes after LFS. Scale bars in (B)–(F), 1 μm.

diameter of the spine head after LFS, and some spines retracted (Figures 1D–1F). Similar to the NMDA-dependent LTD found at hippocampal and cortical synapses (Bear and Malenka, 1994; Bear and Abraham, 1996), we observed persistent reduction in the slope of excitatory postsynaptic potentials (EPSPs, 61.3% ± 10.2% of pre-LFS value at 45–50 min after LFS, n = 10 neurons, Figure 2A) in CA1 pyramidal cells. Furthermore, LTD was absent in neurons that did not received LFS but were imaged repetitively (Figure 2A).

To quantify the extent of spine shrinkage, we measured the diameter of the spine head. The percentage changes of the spine diameter reached a value of 69.6% ± 1.8% at 45 min after LFS (Figure 2B). Further analysis indicated that spine shrinkage, defined as >10% reduction and lasting for at least 30 min in the spine head diameter (see Experimental Procedures), was observed in about 75% of the all spines examined (n = 18 neurons, 7 to 26 spines/neuron, total of 272 spines), while 21% showed shrinkage over the same period of time in the absence of LFS (n = 10 neurons, 9 to 22 spines/neuron, total of 126 spines, see also Figure 4E). In addition, we found that 6.2% of spines in the LFS data set showed shortening by >50%, as compared to 3.2% in the "no stimulation" data set. Furthermore, we noted that LFS-induced reduction of EPSP slope followed a similar time course as that found for the spine shrinkage.

To further analyze activity-induced changes in spine morphology, we quantified the changes in the total fluorescence intensity and volume of the spine head. As shown in Figures 2C and 2D, our results confirmed LFS-induced reduction of the spine size as assayed by the spine head diameter. Furthermore, no significant change in the spine size (diameter, volume, and fluorescence intensity) was observed in the absence of LFS ("No Stim.," Figures 2B–2D) or when the stimulating electrode was placed at a location relatively far (about 100 μm) away from the imaged spines ("Far Stim.," n = 4 neurons, 8 to 19 spines/neuron, total of 53 spines, Figures 2B–2D), suggesting that the observed spine shrinkage was a local effect of stimulation. The absence of changes in the "no stimulation" and "far stimulation" conditions indicates that the reduction in spine size after LFS was not caused by any deleterious effect of two-photon imaging or the whole-cell recording procedure. Finally, we found that the average reduction in the EPSP slope and in the spine size are correlated for a given neuron (n = 15 neurons, Figure 2E). Together with the local nature of the stimulation and spine shrinkage, this correlation supports the notion that the EPSPs recorded were at least partially contributed by activated synapses on the imaged spines.

Spine Head Changes Are Bidirectional and Reversible

It is well established that NMDA-dependent LTD can be readily reversed by subsequent high-frequency stimulation (HFS), which by itself can result in LTP (Bear and Malenka, 1994; Mayford et al., 1995). We thus examined

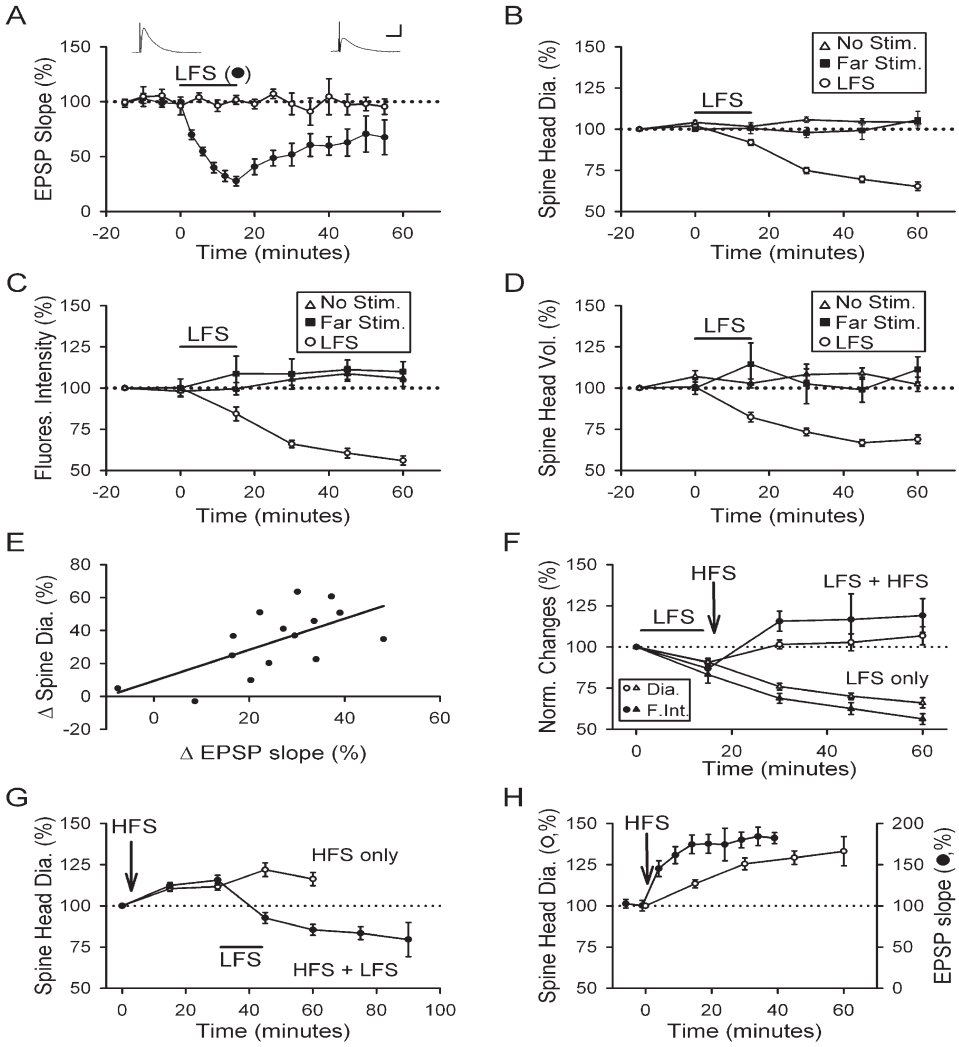

Figure 2. Characterization of Spine Shrinkage Associated with the Induction of LTD

(A) Application of LFS-induced persistent reduction in the synaptic response (filled), as measured by the initial slope of EPSPs, normalized to the average value during the control period prior to LFS. Repetitive imaging, in the absence of LFS, did not alter the slope of the EPSP (open). (Insets) Sample traces from one experiment before (left) and after (right) LFS, average of five consecutive traces around −10 and 45 min. Errors bars, SEM. Scale bars, 20 mS and 2 mV.

(B) Percentage change in the diameter of spine heads following LFS (circles), in the absence of LFS (triangles) or under LFS at a far site (squares). Data were from *all* spines in the image field.

(C and D) Reduction in the fluorescence intensity (C) and spine head volume (D) was observed following LFS applied at a near site (circles) but was not found in the absence of LFS (triangles) or LFS applied at a far site (squares).

(E) Average reduction in the spine diameter correlated with the average reduction in the EPSP slope of the same neuron. The line is a linear fit of all data points.

(F) Application of HFS following LFS reversed the spine shrinkage (LFS + HFS), while the shrinkage persisted when only LFS was applied (LFS only). "Dia," spine head diameter; "F. Int.," fluorescence intensity of the spine head.

(G) Spines showed enlargement after HFS (900 pulses at 100 Hz, open). Subsequent delivery of LFS reversed the spine enlargement and resulted in spine shrinkage (filled).

(H) Induction of LTP (filled) and increase in the spine head diameter (open) after HFS (300 pulses at 100 Hz) in the presence of picrotoxin.

whether spine shrinkage was also susceptible to such a reversal. Indeed, we found that reduction of the spine head induced by LFS was reversed by subsequent HFS (n = 6 neurons, 9 to 15 spines/neuron, total of 76 spines, Figure 2F). This result further suggests that HFS by itself may cause enlargement of the spine head, as has been reported previously (Fifkova and Van Harreveld, 1977; Desmond and Levy, 1983, 1986a; Matsuzaki et al., 2004). When the same number (900) of pulses was delivered at 100 Hz instead of 1 Hz to stimulate presynaptic inputs to CA1 pyramidal cells, we observed a small enlargement of the spine head (Figure 2G), which remained stable when no subsequent stimulation was given (Figure 2G, "HFS only," 116.2% ± 4.0% at 60 min after HFS, n = 7 neurons, 11 to 20 spines/neuron, total of 104 spines). However, if LFS was presented 30 min after HFS, reduction in the size of the spine head occurred (n = 7 neurons, 10 to 15 spines/neuron, total of 82

spines, Figure 2G). Thus, spine size can be bidirectionally regulated, depending on the pattern of synaptic stimulation. In the experiments shown in Figure 2G, HFS was delivered with GABAergic synaptic transmission intact, resulting in a small LTP (112.7% ± 9.5%, 60 min after HFS, n = 7 neurons). To induce a more robust LTP, we applied 300 pulses at 100 Hz in the presence of the GABA receptor blocker picrotoxin (100 μM). A larger increase in the spine size (Figure 2H, 133.1% ± 8.9%, 60 min after HFS, n = 5 neurons, 12 to 21 spines/neuron, total of 93 spines, see also Supplemental Figure S1 [http://www.neuron.org/cgi/content/full/44/5/749/DC1/]) together with a larger LTP (183.2% ± 9.1%, 35–40 min after HFS, n = 5 neurons, Figure 2H) was observed. This result is consistent with previous reports of enlargement of spine size after LTP induction in the hippocampus (Fifkova and Van Harreveld, 1977; Desmond and Levy, 1983, 1986a; Matsuzaki et al., 2004). Taken together, we have shown that the spine head may undergo bidirectional changes in size, depending on the synaptic activity.

LTD and Spine Shrinkage Are Mediated by Divergent Signaling Pathways

Activation of NMDA receptors is required for LFS-induced LTD (Dudek and Bear, 1992; Mulkey and Malenka, 1992). We found that blockade of NMDA receptors by perfusing the slices with the NMDA receptor antagonist APV (50 μM) prevented the spine shrinkage induced by LFS (Figure 3A, 108.2% ± 1.9% in spine diameter or 104.5% ± 5.3% in fluorescence intensity at 30 min after LFS, n = 7 neurons, 8 to 20 spines/neuron, total of 108 spines). After APV was washed out, however, the same set of spines responded to a second LFS with a reduction in size (Figure 3A). Previous studies have shown that elevated activity of calcineurin (PP2B, Mulkey et al., 1994; Hodgkiss and Kelly, 1995) and its downstream effector PP1 is required for LTD (Mulkey et al., 1993; Morishita et al., 2001; see Figure 4G). Preincubation of the slice with FK506, an inhibitor of calcineurin, blocked LTD at these CA1 pyramidal cells (Mulkey et al., 1994; data not shown) and prevented changes in the spine size (Figure 3B, 98.2% ± 2.9% in spine diameter or 102.6% ± 4.2% in fluorescence intensity at 45 min after LFS, n = 7 neurons, 11 to 21 spines/neuron, total of 115 spines). In contrast, preincubation with calyculin A ("CyA") or okadaic acid ("OA"), two PP1/2A inhibitors and potent LTD blockers, did not prevent the LFS-induced spike shrinkage. The average EPSP slope was 107.4% ± 8.4% at 40–45 min after LFS, while the average spine head diameter became 66.5% ± 3.4% (the fluorescence intensity became 63.7% ± 5.1%) of pre-LFS controls at 45 min after LFS (Figure 3C, n = 9 neurons, 10 to 19 spines/neuron, total of 124 spines; p = 0.80, Student's t test, compared to LFS data in Figure 2B). Thus, changes in synaptic responses and spine morphology share common early steps, including activation of NMDA receptors and calcineurin, but diverge in later steps, with PP1 activity required for LTD but not for spine shrinkage.

Cofilin Mediates Spine Shrinkage

What is the downstream target of calcineurin? Dendritic spines are enriched with F-actin, and actin polymerization is known to regulate the spine shape (Sarmiere and Bamburg, 2004). Spine shrinkage is likely to be mediated by actin depolymerization. One of the well-known factors for regulating F-actin is cofilin (Pollard and Borisy, 2003; Bamburg, 1999; Bailly and Jones, 2003), which triggers depolymerization of F-actin and is inactivated by phosphorylation at Ser-3 by LIM kinases. Phosphorylated cofilin (p-cofilin) can be reactivated through dephosphorylation by a family of protein phosphatases, termed Slingshot (Niwa et al., 2002). Interestingly, dendritic spines in CA1 pyramidal cells in mice with deletion of the LIM kinase gene have smaller spine heads (Meng et al., 2002). These smaller spines resemble those observed here following LTD induction. Therefore, we examined whether cofilin activity can mediate spine

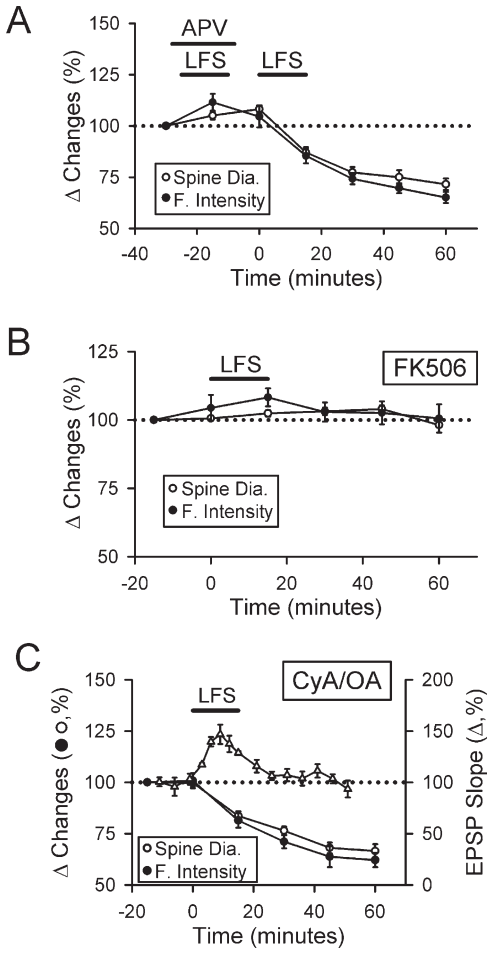

Figure 3. Intracellular Signaling Events Mediating LFS-Induced Spine Shrinkage

(A) Spine shrinkage requires activation of NMDA receptors. No reduction in the diameter (open) or fluorescence intensity (filled) of the spine head was observed when LFS was delivered in the presence of APV. The second LFS, which were delivered after APV was washed out, resulted in spine shrinkage.

(B) Blocking calcineurin activity by preincubation with FK506 prevented the LFS-induced spine shrinkage.

(C) LFS remained effective in reducing the spine diameter (open circles) or fluorescence intensity (filled circles) in slices pretreated with the PP1/2A blocker calyculin A/okadaic acid (CyA/OA), while the reduction in the EPSP slope was completely blocked (triangles).

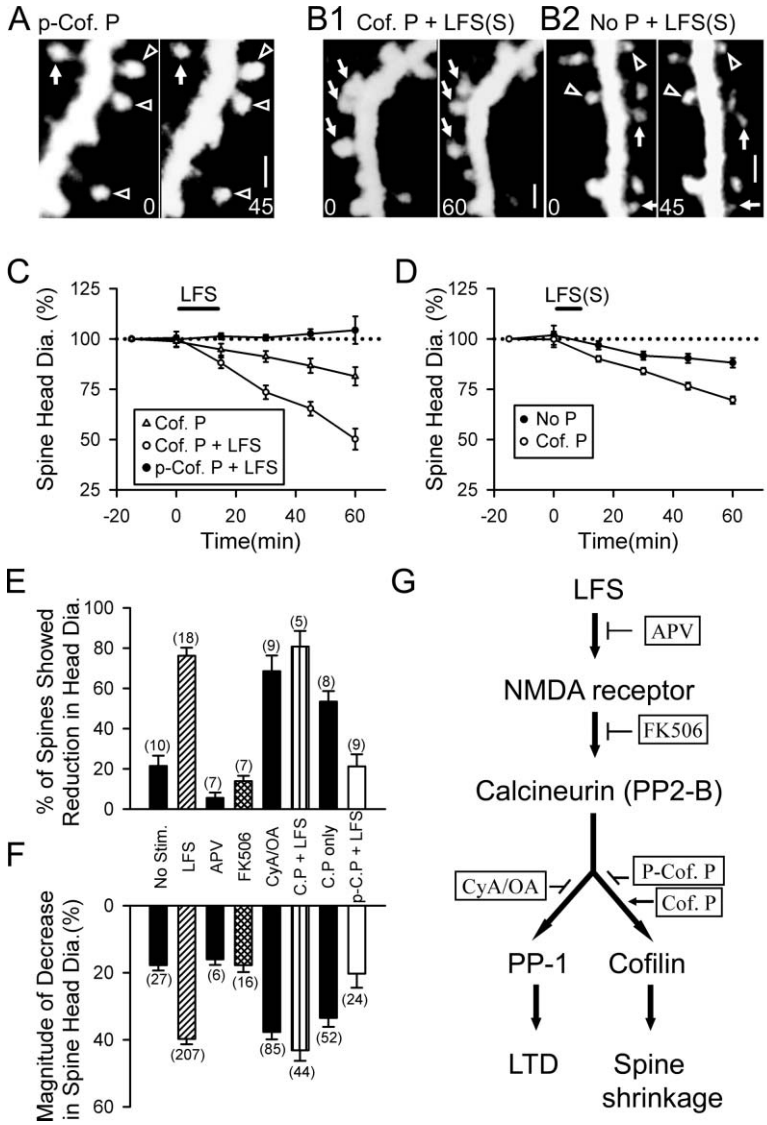

Figure 4. Activity of Cofilin Is Involved in the Spine Shrinkage Associated with LTD

(A) In neurons filled with the p-cofilin peptide, reduction in the spine size was blocked (arrowheads). Note that some spines still underwent small shrinkage (arrow).

(B1 and B2) Neurons loaded with the cofilin peptide showed more marked spine shrinkage induced by 10 min LFS (B1), as compared to nonloaded neurons (B2). Spines that showed clear shrinkage or remain unchanged were marked by arrows or arrowheads, respectively.

(C) P-cofilin peptide blocked spine shrinkage caused by 15 min LFS (p-Cof. P + LFS, filled circles), while cofilin peptide had no apparent effect (Cof. P + LFS, open circles). However, small and gradual spine shrinkage occurred in cells loaded with the cofilin peptide in the absence of stimulation (Cof. P, triangles).

(D) Loading neurons with cofilin peptide enhanced the spine shrinkage induced by 10 min LFS [LFS(S), open] when compared to nonloaded neurons (No P, filled).

(E) The percentage of spines that exhibited significant size reduction (>10%) after LFS. The number refers to the total number of neurons.

(F) The magnitude of reduction in the spine size after LFS. The number refers to the total number of spines from the same set of data in (E).

(G) Proposed signaling pathways that mediate LTD and the spine shrinkage.

shrinkage induced by LFS. Two short peptides (16 amino acids in length) with a sequence corresponding to the N-terminal region of the rat cofilin were synthesized (see Experimental Procedures). One peptide contains a phosphorylated Ser-3 site (termed "p-cofilin peptide"), while the other contains a nonphosphorylated Ser-3 (termed "cofilin peptide"). The synthesized cofilin peptide has been shown to compete effectively with endogenous cofilin as a substrate of LIM kinases, reducing LIM kinase activity and in turn enhancing the activity of endogenous cofilin (Aizawa et al., 2001). On the other hand, the p-cofilin peptide may compete with the endogenous p-cofilin as a substrate for protein phosphatases (e.g., Slingshot), thus preventing the conversion of endogenous p-cofilin into cofilin and spine shrinkage. When hippocampal pyramidal cells were loaded with p-cofilin peptide through the whole-cell recording pipette, LFS-induced spine shrinkage was prevented (Figures 4A and 4C, 102.5% ± 2.3% at 45 min after LFS, n = 9 neurons, 10 to 16 spines/neuron, total of 117 spines). In contrast, in neurons loaded with the cofilin peptide, LFS-induced spine shrinkage occurred to an extent similar to that observed in nonloaded neurons (Figure 4C, 65.3% ± 3.5% at 45 min after LFS, n = 5 neurons, 10 to 12 spines/neurons, total of 55 spines). In the absence of LFS, however, loading cofilin peptide in the neuron led to a gradual spine shrinkage to a lesser extent (86.7% ± 3.6% at 75 min after whole-cell recording, n = 8 neurons, 9 to 20 spines/neuron, total of 97 spines, Figure 4C). Measurement of the fluorescence intensity of the spine head in the above experiments yielded similar results (see Supplemental Figure S2 [http://www.neuron.org/cgi/content/full/44/5/749/DC1/]).

The observations that loading the cofilin peptide induced a small amount of spine shrinkage in the absence of LFS but did not enhance LFS-induced spine shrinkage suggest that the shrinkage process mediated by endogenous cofilin may have been saturated by the 15 min long LFS. If this was the case, the cofilin peptide may enhance spine shrinkage induced by LFS with a shorter duration. We tested the effect of 10 min LFS on neurons loaded with the cofilin peptide. As a control, in inter-

leaved experiments, neurons loaded with normal internal solution were stimulated in the same manner. We found that spine shrinkage was indeed more pronounced in neurons loaded with the cofilin peptide (76.5% ± 1.8% at 45 min after LFS, n = 7 neurons, 12 to 19 spines/neurons, total of 107 spines) than in nonloaded neurons (88.1% ± 2.4% at 45 min after LFS, n = 7 neurons, total of 10 to 16 spines/neurons, total of 96 spines; $p < 0.01$, Student's t test; Figures 4B and 4D). These results further support the notion that cofilin activity mediates spine shrinkage.

The results from all of the experiments on the signaling events underlying spine shrinkage are summarized in Figures 4E and 4F. Under the definition that shrinkage occurred in a particular spine if the reduction of the spine head diameter exceeded 10% and lasted for at least 30 min (see Experimental Procedures), we found a basal rate of spine shrinkage of ~20% in nonstimulated neurons (Figure 4E). Furthermore, we noted that spontaneous shrinkage of spines was not affected in neurons loaded with the p-cofilin peptide (Figure 4E). Interestingly, for those spines that underwent shrinkage, the average percent reduction of the spine head diameter was significantly higher (39%) for those conditions in which LFS was effective in changing spine morphology, as compared to that (18%) of spontaneous shrinkage in nonstimulated neurons or in neurons for which the LFS effect on spine morphology was blocked (Figure 4F). We reached the same conclusion by analyzing the distribution of percent reduction in the spine diameter for the entire population (see Supplemental Figure S3 [http://www.neuron.org/cgi/content/full/44/5/749/DC1/]) instead of focusing on the population of spines that underwent shrinkage, as defined above.

Discussion

In this study, we obtained evidence that dendritic spines undergo marked shrinkage following low-frequency stimulation that induced LTD in the CA1 region of acute hippocampal slices. The most prominent change observed was a reduction of the size of the spine head, although retraction was observed in a small population of spines. The shrinkage of spines was reversed by subsequent high frequency stimulation, which by itself caused enlargement of spine heads and LTP. Activation of NMDA receptors and elevation of calcineurin activity is required for LFS-induced spine shrinkage. However, the shrinkage of spines does not depend on the elevation of PP1 activity, which is required for LTD. Furthermore, we showed that cofilin activity mediates the spine shrinkage induced by LFS.

Repetitive imaging of spines before and after the induction of LTP/LTD allows us to examine morphological changes in the same population of spines. Two separate parameters, the spine head diameter and fluorescence intensity of the spine head, were used to quantify changes in the spine size and yielded the same conclusion on the morphological changes. Several lines of evidence indicate that the spine shrinkage reported here is directly related to the LFS applied to the neuron. First, spine shrinkage was seen only when the synapses were stimulated electrically, and spines distant from the stimulation site were not affected (Figures 1 and 2). Second, the shrinkage depends on the frequency of stimuli. When HFS was given, the spine size was increased rather than decreased (Figure 2 and Supplemental Figure S1 [http://www.neuron.org/cgi/content/full/44/5/749/DC1/]). Third, the LFS-induced spine shrinkage was reversed by subsequent HFS (Figure 2), suggesting that the effect was not due to any deleterious effect caused by the recording, imaging, or stimulation procedures.

We have addressed the signaling events underlying spine shrinkage following LFS. Of particular interest is the finding that loading of the cofilin peptide into these hippocampal neurons enhanced the spine shrinkage induced by a short-duration LFS, while loading of p-cofilin peptide abolished the LFS-induced spine shrinkage (Figure 4). In addition, loading of the cofilin peptide by itself (in the absence of LFS) caused a slight shrinkage of spines (Figure 4). Dephosphorylated cofilin and its close relative actin-depolymerizing factor (ADF) are known to stimulate depolymerization and to sever actin filaments, thus supporting rapid turnover of actin filaments (Sarmiere and Bamburg, 2004). Synthesized cofilin peptide has been shown to compete effectively with endogenous cofilin as a substrate for LIM kinase, thus enhancing the activity of endogenous cofilin (Aizawa et al., 2001). The p-cofilin peptide loaded into the neuron may compete with endogenous p-cofilin and prevent its conversion to active cofilin by endogenous phosphatases, thus abolishing the spine shrinkage induced by LFS. These findings shed light on the function of cofilin in activity-dependent modification of spine morphology in mammalian CNS neurons.

What is the physiological significance of spine shrinkage? An important issue is the relationship between LTD and spine shrinkage. While both processes required activation of NMDA receptor and calcineurin (Figures 3A and 3B), inhibition of a downstream effector PP1 blocked LTD without affecting spine shrinkage (Figure 3C), suggesting divergent downstream pathways leading to LTD and spine shrinkage (Figure 4G). Under physiological conditions, whether these two processes can occur independently remains to be examined. There is evidence that the number of AMPA receptors on a spine is proportional to the area of PSDs and the volume of a spine (Harris and Stevens, 1989; Nusser et al., 1998; Takumi et al., 1999), suggesting that spine morphology and functional synaptic transmission may be coregulated. Such coregulation can result from common upstream processes or through long-term indirect consequences of one process influencing the other. For example, induction of LTD, which causes a reduced number of synaptic AMPA receptors (Carroll et al., 1999; Luscher et al., 1999; Luthi et al., 1999; Wang and Linden, 2000), can result in spine destabilization (Passafaro et al., 2003), perhaps also a reduction in the size of PSD and the spine head. Conversely, spine shrinkage or retraction induced by activity may also lead to further reduction in synaptic efficacy that contributes to the extent of LTD. Over a protracted time course, spine shrinkage and LTD may reinforce each other, leading to synapse elimination. Our experiments were limited to a time scale of about 1 hr and thus cannot provide definitive information on the consequence of morphological changes. However, in the present study, instances of

disappearance of spine heads (Figures 1D and 1F) and retraction of dendritic protrusions (Figures 1D and 1E) have been observed following LFS stimulation. The portion of spines that were retraced after LTD was low (6%), perhaps because a single episode of LTD induction may not be sufficient to trigger spine loss or because the spine loss is a more protracted process. Repeated induction of LTD may exert a cumulative effect on this process of elimination. It will be of interest to determine whether the stable morphology of the spine head is causally related to the presence of PSD, which has been shown to correlate with the stability of filopodial protrusion of the dendrite in slice cultures (Marrs et al., 2001). Activity-induced spine shrinkage over a prolonged period may play an important role in the developmental refinement of neural connections by activity.

Experimental Procedures

Slice Preparation and Electrophysiology

Hippocampal slices (400 μm thick) were prepared from Sprague-Dawley rat pups between P14 and P18 using Vibratome 1000 in cold ACSF containing 110 mM choline chloride, 25 mM $NaHCO_3$, 25 mM D-glucose, 7 mM $MgSO_4$, 2.5 mM KCl, 1.25 mM NaH_2PO_4, 11.6 mM sodium ascorbate, 3.1 mM sodium pyruvate, and 0.5 mM $CaCl_2$. Slices were incubated at 35°C for 30 min before being transferred to a holding chamber at room temperature. The ACSF for holding slices and recording/imaging experiments contained 127 mM NaCl, 2.5 mM KCl, 1.25 mM NaH_2PO_4, 25 mM $NaHCO_3$, 25 mM D-glucose, 2 mM $CaCl_2$, and 1 mM $MgCl_2$. Whole-cell patch recordings were made using borosilicate glass capillaries (Harvard Apparatus) with a resistance of 10–12 MΩ when filled with internal solution containing 128 mM potassium gluconate, 10 mM NaCl, 10 mM Na-HEPES, 0.5 mM EGTA, 2 mM $MgCl_2$, 4 mM Na_2ATP, 0.4 mM NaGTP, and 15 mM phosphocreatine (pH 7.3). To image spines, 1 mM calcein was added to the internal solution. Neurons were kept in current clamp mode after whole-cell configuration was established. To activate synaptic inputs locally, a glass pipette with a 3 μm opening was filled with ACSF and positioned ~20–30 μm away from the imaged spines (Figure 1A). Stimulation strength was adjusted so that the evoked EPSPs recorded at the soma were between 2 and 5 mV. Synaptic activation of spines within the vicinity of the stimulating electrode was confirmed by fluorescent Ca^{2+} imaging (Figure 1B). Test stimuli were given every 20 s to monitor synaptic strength prior to and after LTD induction. A train of 900 pulses at 1 Hz was used to induce LTD. Not every imaging experiment was accompanied by a complete set of physiology data on LTD. In the case that LTD was not monitored continuously, EPSPs were still recorded to ensure that the initial amplitudes were between 2 and 5 mV. Only neurons with resting membrane potentials more negative than −65 mV were used, and experiments were terminated if a neuron's resting potential was more depolarized than −55 mV. All experiments were performed at 32°C ± 1°C.

Peptides with the sequence of MASGVAVSDGVIKVFN (cofilin peptide) or MAS(p)GVAVSDGVIKVFN (p-cofilin peptide) were synthesized and purified with HPLC and were dissolved in the internal solution to the final concentration of 0.5 mM. The patch pipette was tip-filled with 0.5 μl normal internal solution and back-filled with internal solution containing peptide. For pharmacological experiments, slices were incubated with FK506 (1 μM, 1–3 hr) and CyA/OA (1 μM, 30–60 min) before they were transferred to the recording chamber and perfused with normal ACSF. FK506 was a generous gift from Fujisawa Pharmaceutical Cooperation (Japan).

Two-Photon Imaging and Image Analysis

Imaging experiments were performed on a Leica two-photon microscope (DMLFS), using a Tsunami laser (Spectra-Physics) tuned to 890 nm. Fluorescence light was collected with an external photomultiplier. The first set of images was taken 15 min after whole-cell recording was obtained. A region of dendrite (usually of second or third order branches) with ~10 to 20 spines was selected for time-lapse experiments at a higher magnification, using a water-immersion objective (40×, NA 0.8; Leica). The stimulating electrode was then positioned to within 20–30 μm away from the imaged spines. The stimulating electrode was filled with a fluorescent dye, Alexa 594 (20 μM), to visualize its position. Images were taken every 15 min at a resolution of 512 × 512 or 256 × 256 pixels, and the average of two was used in some experiments. For each time point, a stack of images covering the entire 3D range of the spines were taken with a z step size between 0.45 and 0.55 μm. 2D projections of 3D image stacks containing dendritic spines of interest were used for display. To image changes of $[Ca^{2+}]_i$ in the spine, Oregon Green Bapta 488 (200 μM) and Alexa 594 (50 μM) were added to the internal solution with EGTA omitted and the Mg^{2+} concentration in the ACSF lowered to 0.2 mM. Imaging configuration was similar to that described in Oertner et al. (2002), except that BG23 color glass was used to block the red fluorescence of Alexa 594. Images were acquired every 500 ms. To elicite Ca^{2+} elevation in the spine, as shown in Figure 1B, we used a pair of stimuli at 100 Hz, which resulted in two sequential subthreshold EPSPs.

Image analysis was performed blind, without knowing the identity of the samples during the analysis. Dendritic protrusions consist of both spines and filopodia. The majority of the spines can be classified into three types: mushroom, thin, or stubby (see Nimchinsky et al., 2002). Spines were distinguished from filopodia based on two criteria. (1) For thin and mushroom spines, they posses a head that is larger than the rest of the spine. For stubby spines, their diameters (~1 μm) are larger than that of filopodia (<0.5 μm). (2) Spines are in general shorter in length (≤1 μm) than filopodia (≥2 μm). Based on these criteria, spines constitute the major portion (>80%) of the dendritic protrusions we have imaged. To measure the diameter of a spine head, each stack of images was projected to create a 2D image. For mushroom and thin spines, the maximal width of the head was taken as the spine size. For a stubby spine, the width of a spine at halfway between the spine tip and base was taken as its diameter. Diameter measurements were performed using Image J (NIH Image). To measure the volume and fluorescence intensity of the spine head, background fluorescence (at a region free of neuronal structures) was subtracted from the images, and the outline of a spine head was manually drawn for mushroom and thin spines, and the two parameters were measured using MetaMorph analysis program (Universal Imaging). For stubby spines, the volume and fluorescence intensity of the entire spine was measured. Measurements were performed on *all* spines in the image field. All measurements were preformed twice, and the average was used in order to minimize the error. For statistical analysis, we calculated for a given condition the average reduction in the spine diameter over a large number of spines from each experiment on a single neuron (i.e., a single slice), the mean reduction (±SEM) for a number of neurons was determined. The data obtained for the mean reduction (±SEM) was compared between two different experimental conditions, using a Student's t test.

In nonstimulated neurons, the diameter of most spines fluctuated around the basal value. However, the fluctuation was less than 10% of the spine diameter (see Figure 2 and Supplemental Figure S4 [http://www.neuron.org/cgi/content/full/44/5/749/DC1/]). This 10% reduction in spine diameter is close to the optical resolution of our system, thus changes less than 10% were not considered reliable. Consistent with this, we found that, when the reduction in spine diameter was >10%, 67% of them were persistent in the reduction (lasted for at least 30 min), whereas only 18% of those that exhibited <10% reduction were persistent. Therefore, we define that a spine head had undergone significant shrinkage when the reduction in spine head diameter exceeded 10% and the reduction was stable for at least 30 min.

Acknowledgments

This work was supported by NIH (NS37831 and NS36999), National Research Service Awards (to Q.Z.), and the Uehara Memorial Foundation (to K.J.H). We thank Dr. David King for providing synthesized cofilin peptides, and we thank Drs. J. Toshima and Y. Anamizu for helpful discussions.

Received: May 25, 2004
Revised: August 10, 2004
Accepted: October 13, 2004
Published: December 1, 2004

References

Aizawa, H., Wakatsuki, S., Ishii, A., Moriyama, K., Sasaki, Y., Ohashi, K., Sekine-Aizawa, Y., Sehara-Fujisawa, A., Mizuno, K., Goshima, Y., and Yahara, I. (2001). Phosphorylation of cofilin by LIM-kinase is necessary for semaphoring 3A-induced growth cone collapse. Nat. Neurosci. *4*, 367–373.

Andersen, P., and Soleng, A.F. (1998). Long-term potentiation and spatial training are both associated with the generation of new excitatory synapses. Brain Res. Brain Res. Rev. *26*, 353–359.

Bailly, M., and Jones, G.E. (2003). Polarised migration: cofilin holds the front. Curr. Biol. *13*, R128–R130.

Bamburg, J.R. (1999). Proteins of the ADF/cofilin family: essential regulators of actin dynamics. Annu. Rev. Cell Dev. Biol. *15*, 185–230.

Bear, M.F., and Abraham, W.C. (1996). Long-term depression in hippocampus. Annu. Rev. Neurosci. *19*, 437–462.

Bear, M.F., and Malenka, R.C. (1994). Synaptic plasticity: LTP and LTD. Curr. Opin. Neurobiol. *4*, 389–399.

Carroll, R.C., Lissin, D.V., von Zastrow, M., Nicoll, R.A., and Malenka, R.C. (1999). Rapid redistribution of glutamate receptors contributes to long-term depression in hippocampal cultures. Nat. Neurosci. *2*, 454–460.

Chang, F.L., and Greenough, W.T. (1984). Transient and enduring morphological correlates of synaptic activity and efficacy change in the rat hippocampal slice. Brain Res. *309*, 35–46.

Comery, T.A., Harris, J.B., Willems, P.J., Oostra, B.A., Irwin, S.A., Weiler, I.J., and Greenough, W.T. (1997). Abnormal dendritic spines in fragile X knockout mice: maturation and pruning deficits. Proc. Natl. Acad. Sci. USA *94*, 5401–5404.

Dailey, M.E., and Smith, S.J. (1996). The dynamics of dendritic structure in developing hippocampal slices. J. Neurosci. *16*, 2983–2994.

Desmond, N.L., and Levy, W.B. (1983). Synaptic correlates of associative potentiation/depression: an ultrastructural study in the hippocampus. Brain Res. *265*, 21–30.

Desmond, N.L., and Levy, W.B. (1986a). Changes in the numerical density of synaptic contacts with long-term potentiation in the hippocampal dentate gyrus. J. Comp. Neurol. *253*, 466–475.

Desmond, N.L., and Levy, W.B. (1986b). Changes in the postsynaptic density with long-term potentiation in the dentate gyrus. J. Comp. Neurol. *253*, 476–482.

Dudek, S.M., and Bear, M.F. (1992). Homosynaptic long-term depression in area CA1 of hippocampus and effects of N-methyl-D-aspartate receptor blockade. Proc. Natl. Acad. Sci. USA *89*, 4363–4367.

Dunaevsky, A., Tashiro, A., Majewska, A., Mason, C., and Yuste, R. (1999). Developmental regulation of spine motility in the mammalian central nervous system. Proc. Natl. Acad. Sci. USA *96*, 13438–13443.

Engert, F., and Bonhoeffer, T. (1999). Dendritic spine changes associated with hippocampal long-term synaptic plasticity. Nature *399*, 66–70.

Ferrer, I., and Gullotta, F. (1990). Down's syndrome and Alzheimer's disease: dendritic spine counts in the hippocampus. Acta Neuropathol. (Berl.) *79*, 680–685.

Fiala, J.C., Feinberg, M., Popov, V., and Harris, K.M. (1998). Synaptogenesis via dendritic filopodia in developing hippocampal area CA1. J. Neurosci. *18*, 8900–8911.

Fifkova, E., and Anderson, C.L. (1981). Stimulation-induced changes in dimensions of stalks of dendritic spines in the dentate molecular layer. Exp. Neurol. *74*, 621–627.

Fifkova, E., and Van Harreveld, A. (1977). Long-lasting morphological changes in dendritic spines of dentate granular cells following stimulation of the entorhinal area. J. Neurocytol. *6*, 211–230.

Geinisman, Y. (2000). Structural synaptic modifications associated with hippocampal LTP and behavioral learning. Cereb. Cortex *10*, 952–962.

Harris, K.M. (1999). Structure, development, and plasticity of dendritic spines. Curr. Opin. Neurobiol. *9*, 343–348.

Harris, K.M., and Stevens, J.K. (1989). Dendritic spines of CA 1 pyramidal cells in the rat hippocampus: serial electron microscopy with reference to their biophysical characteristics. J. Neurosci. *9*, 2982–2997.

Hodgkiss, J.P., and Kelly, J.S. (1995). Only 'de novo' long-term depression (LTD) in the rat hippocampus in vitro is blocked by the same low concentration of FK506 that blocks LTD in the visual cortex. Brain Res. *705*, 241–246.

Jacobs, B., Driscoll, L., and Schall, M. (1997). Life-span dendritic and spine changes in areas 10 and 18 of human cortex: a quantitative Golgi study. J. Comp. Neurol. *386*, 661–680.

Lee, K.S., Schottler, F., Oliver, M., and Lynch, G. (1980). Brief bursts of high-frequency stimulation produce two types of structural change in rat hippocampus. J. Neurophysiol. *44*, 247–258.

Luscher, C., Xia, H., Beattie, E.C., Carroll, R.C., von Zastrow, M., Malenka, R.C., and Nicoll, R.A. (1999). Role of AMPA receptor cycling in synaptic transmission and plasticity. Neuron *24*, 649–658.

Luthi, A., Chittajallu, R., Duprat, F., Palmer, M.J., Benke, T.A., Kidd, F.L., Henley, J.M., Isaac, J.T., and Collingridge, G.L. (1999). Hippocampal LTD expression involves a pool of AMPARs regulated by the NSF-GluR2 interaction. Neuron *24*, 389–399.

Maletic-Savatic, M., Malinow, R., and Svoboda, K. (1999). Rapid dendritic morphogenesis in CA1 hippocampal dendrites induced by synaptic activity. Science *283*, 1923–1927.

Marrs, G.S., Green, S.H., and Dailey, M.E. (2001). Rapid formation and remodeling of postsynaptic densities in developing dendrites. Nat. Neurosci. *4*, 1006–1013.

Matsuzaki, M., Honkura, N., Ellis-Davies, G.C., and Kasai, H. (2004). Structural basis of long-term potentiation in single dendritic spines. Nature *429*, 761–766.

Mayford, M., Wang, J., Kandel, E.R., and O'Dell, T.J. (1995). CaMKII regulates the frequency-response function of hippocampal synapses for the production of both LTD and LTP. Cell *81*, 891–904.

Meng, Y., Zhang, Y., Tregoubov, V., Janus, C., Cruz, L., Jackson, M., Lu, W.Y., MacDonald, J.F., Wang, J.Y., Falls, D.L., and Jia, Z. (2002). Abnormal spine morphology and enhanced LTP in LIMK-1 knockout mice. Neuron *35*, 121–133.

Morishita, W., Connor, J.H., Xia, H., Quinlan, E.M., Shenolikar, S., and Malenka, R.C. (2001). Regulation of synaptic strength by protein phosphatase 1. Neuron *32*, 1133–1148.

Moser, M.B., Trommald, M., and Andersen, P. (1994). An increase in dendritic spine density on hippocampal CA1 pyramidal cells following spatial learning in adult rats suggests the formation of new synapses. Proc. Natl. Acad. Sci. USA *91*, 12673–12675.

Mulkey, R.M., and Malenka, R.C. (1992). Mechanisms underlying induction of homosynaptic long-term depression in area CA1 of the hippocampus. Neuron *9*, 967–975.

Mulkey, R.M., Herron, C.E., and Malenka, R.C. (1993). An essential role for protein phosphatases in hippocampal long-term depression. Science *261*, 1051–1055.

Mulkey, R.M., Endo, S., Shenolikar, S., and Malenka, R.C. (1994). Involvement of calcineurin/inhibitor-1 phosphatase cascade in hippocampal long-term depression. Nature *369*, 486–488.

Nimchinsky, E.A., Sabatini, B.L., and Svoboda, K. (2002). Structure and function of dendritic spines. Annu. Rev. Physiol. *64*, 313–353.

Niwa, R., Nagata-Ohashi, K., Takeichi, M., Mizuno, K., and Uemura, T. (2002). Control of actin reorganization by Slingshot, a family of phosphatases that dephosphorylate ADF/cofilin. Cell *108*, 233–246.

Nusser, Z., Lujan, R., Laube, G., Roberts, J.D., Molnar, E., and Somogyi, P. (1998). Cell type and pathway dependence of synaptic AMPA receptor number and variability in the hippocampus. Neuron *21*, 545–559.

Oertner, T.G., Sabatini, B.L., Nimchinsky, E.A., and Svoboda, K. (2002). Facilitation at single synapses probed with optical quantal analysis. Nat. Neurosci. *5*, 657–664.

O'Malley, A., O'Connell, C., Murphy, K.J., and Regan, C.M. (2000). Transient spine density increases in the mid-molecular layer of hippocampal dentate gyrus accompany consolidation of a spatial learning task in the rodent. Neuroscience *99*, 229–232.

Passafaro, M., Nakagawa, T., Sala, C., and Sheng, M. (2003). Induction of dendritic spines by an extracellular domain of AMPA receptor subunit GluR2. Nature *424*, 677–681.

Pollard, T.D., and Borisy, G.G. (2003). Celluar motility driven by assembly and disassembly of actin filaments. Cell *112*, 453–465.

Sarmiere, P.D., and Bamburg, J.R. (2004). Regulation of the neuronal actin cytoskeleton by ADF/cofilin. J. Neurobiol. *58*, 103–117.

Sorra, K.E., and Harris, K.M. (1998). Stability in synapse number and size at 2 hr after long-term potentiation in hippocampal area CA1. J. Neurosci. *18*, 658–671.

Takumi, Y., Ramirez-Leon, V., Laake, P., Rinvik, E., and Ottersen, O.P. (1999). Different modes of expression of AMPA and NMDA receptors in hippocampal synapses. Nat. Neurosci. *2*, 618–624.

Uemura, E. (1980). Age-related changes in prefrontal cortex of Macaca mulatta: synaptic density. Exp. Neurol. *69*, 164–172.

Wang, Y.T., and Linden, D.J. (2000). Expression of cerebellar long-term depression requires postsynaptic clathrin-mediated endocytosis. Neuron *25*, 635–647.

White, E.L., Weinfeld, L., and Lev, D.L. (1997). A survey of morphogenesis during the early postnatal period in PMBSF barrels of mouse SmI cortex with emphasis on barrel D4. Somatosens. Motil. Res. *14*, 34–55.

Wise, S.P., Fleshman, J.W., Jr., and Jones, E.G. (1979). Maturation of pyramidal cell form in relation to developing afferent and efferent connections of rat somatic sensory cortex. Neuroscience *4*, 1275–1297.

Yuste, R., and Bonhoeffer, T. (2004). Genesis of dendritic spines: insights from ultrastructural and imaging studies. Nat. Rev. Neurosci. *5*, 24–34.